Nonequilibrium phase transition in a non-integrable zero-range process

2006 J. Phys. A: Math. Gen. 39 9055

(http://iopscience.iop.org/0305-4470/39/29/003)

INSTITUTE OF PHYSICS PUBLISHING JOURNAL OF PHYSICS A: MATHEMATICAL AND GENERAL

J. Phys. A: Math. Gen. **39** (2006) 9055–9069 doi:10.1088/0305-4470/39/29/003

Nonequilibrium phase transition in a non-integrable zero-range process

C Godrèche

Isaac Newton Institute for Mathematical Sciences, 20 Clarkson Road, Cambridge, CB3 0EH, UK
and
Service de Physique de l'État Condensé, CEA Saclay, 91191 Gif-sur-Yvette cedex, France

Received 9 March 2006, in final form 24 May 2006
Published 5 July 2006
Online at stacks.iop.org/JPhysA/39/9055

Abstract

The present work is an endeavour to determine analytically features of the stationary measure of a non-integrable zero-range process, and to investigate the possible existence of phase transitions for such a nonequilibrium model. The rates defining the model do not satisfy the constraints necessary for the stationary measure to be a product measure. Even in the absence of a drive, detailed balance with respect to this measure is violated. Analytical and numerical investigations on the complete graph demonstrate the existence of a first-order phase transition between a fluid phase and a condensed phase, where a single site has macroscopic occupation. The transition is sudden from an imbalanced fluid where both species have densities larger than the critical density, to a critical neutral fluid and an imbalanced condensate.

PACS number: 64.60.−i

(Some figures in this article are in colour only in the electronic version)

1. Introduction

Zero-range processes (ZRP) are minimal models [1], often used as simplified realizations of more complex processes (for reviews, see [2–4]). For instance they are instrumental for the understanding of condensation transitions in driven diffusive systems [5, 6]. They are closely related to urn models, which themselves are simplified models of a number of stochastic processes in physics [8]. In a ZRP, particles, all equivalent, hop from sites to sites on a lattice, with prescribed rates which only depend on the occupation of the departure site. The fundamental property of this process is that the stationary measure is explicitly known as a function of the rates, and is a product measure [1, 7].

A natural generalization of this definition is when two different species are allowed to coexist on each site, again hopping with prescribed rules. However in this case the stationary measure is a product measure only if the rates with which the particles of both species leave

a given site satisfy a constraint [9, 10] (see equation (2.5) below). For short, we refer to ZRP satisfying (2.5) as *integrable*. If these rates do not satisfy the constraints, the stationary measure is not known, and the corresponding ZRP is a generic nonequilibrium model: it violates detailed balance, even in the absence of a drive applied to the system, as will be shown below. A question of fundamental importance posed by the study of nonequilibrium systems is the nature of their stationary state, and in particular the possible existence of phase transitions at stationarity.

The present work is devoted to the investigation of this question on the particular example of a non-integrable two-species ZRP. The model arose from the study of a two-species driven diffusive system (DDS) exhibiting, at stationarity, condensation with coexistence between a high and a low density phase in each individual domain [6]. A domain in the original DDS, i.e. a stretch of particles of the two species, corresponds to a site in the ZRP, while the high and low density phases correspond to the two species of the ZRP.

We study the model on the complete graph (i.e., in the fully connected geometry), using analytical and numerical methods. While for equal densities of the two species the transition between a fluid phase and a condensed phase is continuous (as is the case for the corresponding single-species ZRP), for nonequal densities this transition is discontinuous. The model exhibits a sudden phase transition from an imbalanced fluid where both species have densities larger than the critical density to a neutral fluid, with densities of both species equal to the critical density, and an imbalanced condensate. As a consequence re-entrance is observed. The system is successively fluid, condensed, fluid, when increasing the density of one species, holding the density of the other species fixed. Coexistence between the two phases takes place along the transition line only. This study can serve as a template for the study of the one-dimensional model.

2. Definition of the model

2.1. A reminder on zero-range processes

We first give a short reminder of the definition of a ZRP. Consider, in any dimension, a lattice of M sites on which N particles are moving. Multiple occupancy of a site is allowed. The dynamics consists in choosing a site at random, then transferring one of the particles present on this site, to an arrival site. On the complete graph all sites are connected. The arrival site is any site chosen randomly. In one dimension, the arrival site is one of the two nearest neighbours, chosen with a given probability, p, to the right, or $q = 1 - p$, to the left. The transfer of particles is done with the rate u_k ($k > 0$), only depending on the number k of particles on the departure site.

The fundamental property of the ZRP is that its stationary measure is known, and is a product measure, as follows. Let us denote by N_i the random occupation of site i. The stationary weight of a configuration of the system is

$$\mathcal{P}(N_1, \ldots, N_M) = \frac{1}{Z_{M,N}} \prod_{i=1}^{M} p_{N_i} \delta\left(\sum_i N_i, N\right), \tag{2.1}$$

where the normalization factor $Z_{M,N}$ reads

$$Z_{M,N} = \sum_{N_1} \cdots \sum_{N_M} p_{N_1} \cdots p_{N_M} \delta\left(\sum_i N_i, N\right). \tag{2.2}$$

For a given rate u_k, the factors p_k obey the relation

$$u_k p_k = p_{k-1} \tag{2.3}$$

which leads to the explicit form

$$p_0 = 1, \qquad p_k = \frac{1}{u_1 \dots u_k}. \tag{2.4}$$

Let us emphasize two important characteristics of the ZRP (the same holding for integrable two-species ZRP, defined below).

- When the dynamics is symmetric, e.g. in the one-dimensional geometry with $p = 1/2$, or in the fully connected geometry, detailed balance with respect to the stationary measure is satisfied. For the single-species ZRP the detailed balance condition reads

  $$p_k p_l u_k = p_{k-1} p_{l+1} u_{l+1},$$

  which is precisely the property that leads to (2.3).[1]
- As can be seen on (2.1), the stationary measure is independent of the asymmetry. As a consequence, any property of the ZRP based on the sole knowledge of this measure is itself independent of the asymmetry. For example, with special choices of the transfer rate u_k, a condensation transition can occur in the system. The features characterizing this phase transition are independent of the asymmetry.

This is in contrast with the ZRP studied in the present work, where detailed balance is *not* satisfied, *even when the dynamics is symmetric*, i.e., in the absence of a drive, as explained below. In this sense this model is a generic nonequilibrium model, and the phase transition described in the next sections is specific of a nonequilibrium system.

2.2. The model considered in the present work

The model considered in the present work is a two-species ZRP. The general definition of a two-species ZRP is a simple extension of that of the usual ZRP [9, 10]. Consider, in any dimension, a lattice of M sites with n particles of type 1, m particles of type 2. The dynamics consists in choosing a site at random, then transferring one of the particles present on this site, of one of the species chosen at random, to an arrival site. The transfer of particles is done with rates $u_{k,l}$ ($k > 0$) for a particle of the first species, and $v_{k,l}$ ($l > 0$) for a particle of the other species, where k and l are respectively the number of particles of each species on the departure site.

At variance with the case of single-species ZRP where the stationary measure is a product measure for any choice of the transfer rate, for a two-species ZRP this property holds only if the following constraint on the rates $u_{k,l}$ and $v_{k,l}$ is satisfied [9, 10]:

$$u_{k,l} v_{k-1,l} = v_{k,l} u_{k,l-1}. \tag{2.5}$$

In the present work we choose rates which violate this constraint. As a consequence, nothing *a priori* is known on the nature of the stationary measure of the model. The rates read

$$u_{k,l} = 1 + \frac{b}{l}, \qquad v_{k,l} = 1 + \frac{b}{k}, \tag{2.6}$$

where b is a given parameter, which plays the role of inverse temperature [4]. We also set $u_{k,0} = v_{0,l} = 1 + b$ in order to complete the definition of the process. These rates favour equality of the number of particles of both species on each site. This choice aims at reproducing a feature of the original DDS, where inside the domains coexistence between a high and a low density phase takes place. The model was first introduced in [6], and studied in the equal density case. This is reviewed and extended below. We then focus on the nonequal density case.

[1] When the dynamics is not symmetric, the condition of detailed balance is replaced by a condition of pairwise balance. See [4] for a discussion of this point.

3. The case of two sites

We begin by considering the case where the system is made of two sites. This case shares many common features with the complete model and serves as a useful preparation for the rest.

A configuration of the system is entirely specified by the numbers k and l of particles of each species on site 1, since the number of particles on site 2 are then just equal to $n-k$ and $m-l$. Therefore the weight of a configuration of the system is given by the probability $f_{k,l}(t)$ that site 1 contains k particles of one species, and l particles of the other species, at time t. It obeys the master equation

$$\frac{\mathrm{d}f_{k,l}(t)}{\mathrm{d}t} = u_{k+1,l}f_{k+1,l}(1-\delta_{k,n}) + v_{k,l+1}f_{k,l+1}(1-\delta_{l,m}) + u_{n-k+1,m-l}f_{k-1,l}(1-\delta_{k,0}) + v_{n-k,m-l+1}f_{k,l-1}(1-\delta_{l,0}) - [u_{k,l}+v_{k,l}+u_{n-k,m-l}+v_{n-k,m-l}]f_{k,l},$$

where it is understood that $u_{0,l} = v_{k,0} = 0$. This is the master equation of a biased random walk in the rectangle $0 \leqslant k \leqslant n, 0 \leqslant l \leqslant m$, with reflecting boundary conditions.

We would like to know the stationary solution $f_{k,l}$ of this equation, for *any choice of rates* $u_{k,l}$, $v_{k,l}$. It turns out that this question is already too hard to answer for the seemingly simple problem of a two-site model. We must content ourselves of the knowledge of the stationary solution for the class of processes fulfilling the constraint (2.5). Indeed, proviso the rates fulfil this constraint, the stationary distribution is given by

$$f_{k,l} = \frac{p_{k,l}p_{n-k,m-l}}{Z_{M,n,m}}, \tag{3.1}$$

where

$$p_{k,l}u_{k,l} = p_{k-1,l}, \qquad p_{k,l}v_{k,l} = p_{k,l-1}, \tag{3.2}$$

and $Z_{M,n,m}$ is a normalization (the partition function). Relations (3.2) can be iterated, thus determining the $p_{k,l}$ in terms of the rates. Equations (3.1) and (3.2) generalize equations (2.1) and (2.3).

These results can be obtained by making the ansatz (3.1), carry this form into the master equation, which then leads to (3.2). Equation (2.5) appears as a compatibility relation for (3.2) [9, 10].

Let us consider this issue from a complementary viewpoint. We note first that the dynamics between the two sites is symmetric. We then question the possibility for the process to be reversible in time, and investigate the consequences thereby. Reversibility is equivalently the property that the process obeys detailed balance with respect to the stationary measure, or otherwise stated that the system is at equilibrium.

(i) Let us determine the stationary distribution $f_{k,l}$ when detailed balance is obeyed. Consider the transitions from $\{k,l\}$ to $\{k+1,l\}$ and back, and from $\{k,l\}$ to $\{k,l+1\}$ and back. Detailed balance requires

$$u_{n-k,m-l}f_{k,l} = u_{k+1,l}f_{k+1,l}, \qquad v_{n-k,m-l}f_{k,l} = v_{k,l+1}f_{k,l+1}.$$

It is readily found that a solution of these equations is given by (3.1) and (3.2).

(ii) Let us now show how (2.5) is related to reversibility by yet another path. We use the Kolmogorov criterion [11, 12] which is a necessary and sufficient condition for a Markov process to be reversible. This condition states that the product of the transition rates along any cycle in the space of configurations should be equal to the product of the transition rates for the reverse cycle. In the present case, the space of configurations is the rectangle $0 \leqslant k \leqslant n, 0 \leqslant l \leqslant m$. Taking the cycle

$$(k,l) \to (k,l-1) \to (k+1,l-1) \to (k+1,l) \to (k,l),$$

then the cycle in reverse order, the Kolmogorov condition leads to the equation

$$\frac{u_{k+1,l}\,v_{k,l}}{u_{k+1,l-1}\,v_{k+1,l}} = \frac{u_{n-k,m-l}\,v_{n-k,m-(l-1)}}{u_{n-k,m-(l-1)}\,v_{n-(k+1),m-(l-1)}}. \tag{3.3}$$

This equation is satisfied if (2.5) holds[2].

To summarize, reversibility implies stationary product measure, equations (3.1), (3.2), and a constraint on the rates, equation (2.5). The reciprocal statement holds. The proof follows easily from the fact that a Markov process with a finite configuration space has a unique stationary solution. We leave it to the reader.

The physical interpretation of the results above is that when the system is at equilibrium, its energy is equal to the sum of the energies of two independent sites.

Conversely, for a choice of rates violating (2.5), as is the case for the model studied here, the model is not reversible, the stationary measure does not take the simple form (3.1), and is not known *a priori*. In other words, for a general choice of rates, the two-site model can have an arbitrarily complex stationary measure. In this sense it represents an example of a minimal nonequilibrium system. One can think of it as some kind of generalization of the Ehrenfest urn model.

4. The model on the complete graph

The virtue of considering the fully connected geometry, in the thermodynamical limit of an infinite system, is that it leads to analytical results on the model. The rest of the paper is devoted to this case.

Consider again the single-site occupation probability $f_{k,l}(t)$, that is the probability that a generic site contains k particles of one species, and l particles of the other species, at time t. Conservation of probability and particle numbers imposes $\sum_{k,l} f_{k,l}(t) = 1$ and

$$\sum_{k=1}^{\infty} k f_k(t) = \rho_1, \qquad \sum_{l=1}^{\infty} l f_l(t) = \rho_2, \tag{4.1}$$

where for a large system, densities are defined as $\rho_1 = n/M$, $\rho_2 = m/M$, and where the marginals are denoted by $f_k = \sum_l f_{k,l}$, and $f_l = \sum_k f_{k,l}$.

The master equation for the temporal evolution of $f_{k,l}(t)$ reads

$$\begin{aligned}\frac{\mathrm{d}f_{k,l}(t)}{\mathrm{d}t} &= u_{k+1,l}\,f_{k+1,l} + v_{k,l+1}\,f_{k,l+1} + \bar{u}_t\,f_{k-1,l}(1-\delta_{k,0}) \\ &\quad + \bar{v}_t\,f_{k,l-1}(1-\delta_{l,0}) - [u_{k,l} + v_{k,l} + \bar{u}_t + \bar{v}_t]\,f_{k,l},\end{aligned} \tag{4.2}$$

where

$$\bar{u}_t = \sum_{k,l} u_{k,l}\,f_{k,l}, \qquad \bar{v}_t = \sum_{k,l} v_{k,l}\,f_{k,l}$$

are the mean rates at which a particle arrives on a site $(k \to k+1)$ or $(l \to l+1)$. Equation (4.2) is the master equation for a biased random walk in the quadrant $k, l \geqslant 0$, with reflecting boundary conditions on the axes.

[2] Equation (3.3) can be satisfied by imposing symmetry relations on the rates:

$$u_{k+1,l} = u_{n-k,m-l}, \qquad v_{k,l+1} = v_{n-k,m-l}.$$

The corresponding stationary measure is uniform:

$$f_{k,l} = \frac{1}{(n+1)(m+1)},$$

and detailed balance is obeyed. We discard this solution because the rates would then also depend on the arrival site.

We wish to determine the stationary solution of this equation. We follow the same line of thought as in the previous section. We show that the stationary distribution $f_{k,l}$ has a known closed-form expression only if reversibility is assumed. Indeed, using the detailed balance conditions

$$f_{k+1,l}u_{k+1,l} = \bar{u}\, f_{k,l}, \qquad f_{k,l+1}v_{k,l+1} = \bar{v}\, f_{k,l},$$

it is easy to derive the following explicit expression for the stationary distribution $f_{k,l}$:

$$f_{k,l} = \frac{p_{k,l}\bar{u}^k\bar{v}^l}{\sum_{k,l} p_{k,l}\bar{u}^k\bar{v}^l}, \tag{4.3}$$

where the $p_{k,l}$ are given by (3.2), and $\bar{u}$ and $\bar{v}$ are the stationary mean hopping rates. The latter are determined by the sum rules (4.1), and play the role of fugacities in the grand canonical formalism [3].

Let us also show that, as for the two-site system, the constraint (2.5) is a consequence of imposing reversibility. Indeed, the space of configurations is the quadrant $k, l \geqslant 0$. Taking the cycle

$$(k, l) \to (k, l-1) \to (k+1, l-1) \to (k+1, l) \to (k, l),$$

then the cycle in reverse order, the Kolmogorov condition implies

$$v_{k,l}\bar{u}\bar{v}u_{k+1,l} = \bar{u}v_{k+1,l}u_{k+1,l-1}\bar{v},$$

which yields (2.5).

As for the two-site system, we conclude that conversely, when (2.5) is violated, as is the case with the choice of rates (2.6), the stationary distribution remains unknown. The present work is an endeavour to determine features of the stationary measure of the model for a thermodynamical system, and to investigate the possible existence of nonequilibrium phase transitions.

In the case of an integrable two-species ZRP, the fugacities are functions of the densities (see equation (4.3)). The duality fugacity density is replaced here by the duality mean hopping rate density.

5. Criticality

As will appear clearly as we proceed, the critical point for this model is unique, and corresponds to taking $\bar{u} = \bar{v} = 1$.

5.1. Continuum limit: universal properties

Let us first consider the continuum limit of the stationary equation, in the asymptotic regime where k and l are large, and setting $\bar{u} = \mathrm{e}^{\mu}$, $\bar{v} = \mathrm{e}^{\nu}$, where μ and ν are small. Expanding $f_{k,l}$ to second order, we obtain

$$\frac{\partial^2 f_{k,l}}{\partial k^2} + \frac{\partial^2 f_{k,l}}{\partial l^2} + \frac{\partial f_{k,l}}{\partial k}\left(\frac{b}{l} - \mu\right) + \frac{\partial f_{k,l}}{\partial l}\left(\frac{b}{k} - \nu\right) = 0. \tag{5.1}$$

At criticality, i.e. when $\mu = \nu = 0$, equation (5.1) becomes scale invariant, and reads

$$\frac{\partial^2 f_{k,l}}{\partial k^2} + \frac{\partial^2 f_{k,l}}{\partial l^2} + b\left(\frac{1}{l}\frac{\partial f_{k,l}}{\partial k} + \frac{1}{k}\frac{\partial f_{k,l}}{\partial l}\right) = 0. \tag{5.2}$$

Using polar coordinates: $k = r\cos\theta, l = r\sin\theta$, with $0 \leqslant \theta \leqslant \pi/2$, this equation is transformed into

$$\frac{\partial^2 f(r,\theta)}{\partial r^2} + \frac{1}{r^2}\frac{\partial^2 f(r,\theta)}{\partial \theta^2} + \frac{1}{r}\frac{\partial f(r,\theta)}{\partial r}\left(1 + \frac{2b}{\sin 2\theta}\right) = 0. \tag{5.3}$$

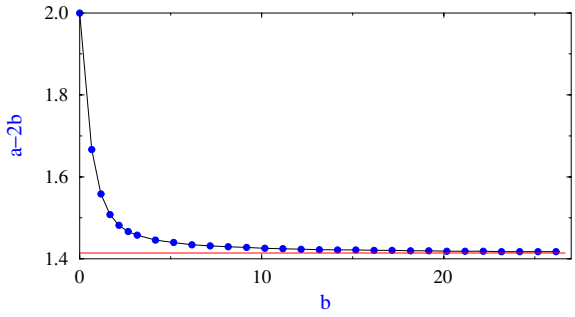

Figure 1. Decay exponent a as a function of b. At large values of b, $a \approx 2b + \sqrt{2}$.

Now, setting $f(r,\theta) = r^{-a} g(\theta)$, we find an equation for the angular function $g(\theta)$:

$$\frac{\mathrm{d}^2 g(\theta)}{\mathrm{d}\theta^2} + a\left(a - \frac{2b}{\sin 2\theta}\right) g(\theta) = 0. \tag{5.4}$$

The unknown decay exponent a is determined by the boundary conditions imposed on $g(\theta)$, which are the quantization conditions of this Schrödinger equation. Indeed, $g(\theta)$ is positive for $0 \leqslant \theta \leqslant \pi/2$, symmetric with respect to $\pi/4$ and must vanish for $\theta = 0$ or $\theta = \pi/2$. For special values of b, exact solutions of equations (5.3) can be found:

$$f(r,\theta) = r^{-2} \sin\theta \cos\theta \qquad (b = 0), \tag{5.5}$$

$$f(r,\theta) = r^{-3} \sin\theta \cos\theta (\sin\theta + \cos\theta) \qquad (b = 2/3). \tag{5.6}$$

For $b = 0$ the original model has no critical behaviour, hence formally $a = 0$. On the other hand the prediction of the continuum limit for the decay exponent, in the limit $b \to 0$, is $a = 2$. The decay exponent a is discontinuous at $b = 0$.

For a generic value of b, the decay exponent a is determined by numerical integration of the differential equation (5.4). At large values of b, the behaviour of this exponent can be obtained analytically. Indeed, expanding the potential term in (5.4) to second order around its minimum, located at $\pi/4$, yields the equation of a harmonic oscillator, with coupling constant $\omega = 2\sqrt{ab}$ and energy $a(a-2b)/2$:

$$g''(x) + a(a - 2b - 4bx^2) g(x) = 0,$$

where $x = \pi/4 - \theta$. Imposing that the ground state energy be equal to $\omega/2$ yields the asymptotic quantization condition $a = 2b + \sqrt{2}$. (See figure 1.)

As a consequence, we find the remarkable result that, at criticality, the marginal distributions f_k and f_l decay as power laws at large occupations, with a non-trivial exponent equal to $a - 1$. The same holds for p_m, with $m = k + l$, the distribution of the total number of particles on a site,

$$p_m = \sum_{k=0}^{m} f_{k,m-k} \sim m^{-(a-1)}.$$

As is clear from the treatment presented above, both the function $g(\theta)$ and the exponent a are universal. They are determined by the large k, l behaviour of the rates and of $f_{k,l}$, and thus only depend on b. The common critical density ρ_c of both species (see below) is a non-universal quantity. It depends on the details of the rates and on the value of $f_{k,l}$ for finite k and l.

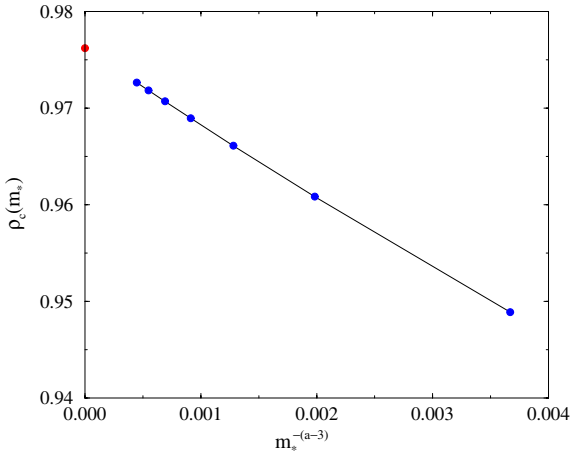

Figure 2. Determination of the critical density by extrapolation of the data for $m_\star = 40, 60, \ldots, 160$. The circle on the vertical axis is the extrapolated value for ρ_c. ($b = 3/2, a = 4.520\ldots, \bar{u} = \bar{v} = 1$.)

5.2. Discrete equations: critical density

The determination of the non-universal critical density ρ_c of both species, where

$$\rho_c = \sum_{k=1}^{\infty} k f_k = \sum_{l=1}^{\infty} l f_l, \qquad (\bar{u} = \bar{v} = 1),$$

requires the knowledge of the stationary solution $f_{k,l}$ of the discrete equations (4.2). These are integrated numerically with $\bar{u} = \bar{v} = 1$, using the following method. We truncate these equations at a given value of $k + l$ denoted by $m_\star$, which plays the role of a cut-off. We solve the linear system $AF = I$, where F is the column matrix of the occupation probabilities $f_{k,l}$, I is the matrix containing the inhomogeneous term $f_{0,0}$, itself determined at the end of the computation by normalization, and A is the matrix deduced from the stationary equations. We impose the boundary conditions $f_{k,l} = 0$ outside the triangle delimited by $k = 0, l = 0$ and $k + l = m_\star$. The maximal value of the cut-off $m_\star$ attainable is limited by the size of the matrices involved. For example, taking $m_\star = 160$ corresponds to a linear system of order 13 040.

As an illustration we take $b = 3/2$, corresponding to a value of the decay exponent $a \approx 4.520$. Extrapolating the data for several values of $m_\star$, using the estimate

$$\rho_c - \rho_c(m_\star) \approx \int_{m_\star}^{\infty} \mathrm{d}m\, m p_m \sim m_\star^{-(a-3)},$$

as depicted in figure 2, leads to $\rho_c \approx 0.976$.

The theoretical prediction for the critical decay exponent of p_m, or $f_k \equiv f_l$, agrees perfectly well with numerical measurements.

6. Fluid phase

For non-zero values of μ and ν the system is driven away from criticality. We begin by investigating exponentially decreasing solutions of the continuum limit stationary

equation (5.1). We then study the stationary solutions of the discrete equation (4.2). We finally determine the region of existence of such solutions.

6.1. Stationary solutions at exponential order: continuum limit

If we content ourselves of the knowledge of the stationary solutions at exponential order, that is retaining their exponential dependence only, and discarding any prefactor, then terms containing b can be neglected. Equation (5.1) now reads

$$\frac{\partial^2 f_{k,l}}{\partial k^2} + \frac{\partial^2 f_{k,l}}{\partial l^2} - \mu \frac{\partial f_{k,l}}{\partial k} - \nu \frac{\partial f_{k,l}}{\partial l} = 0. \tag{6.1}$$

Setting $f_{k,l} = \mathrm{e}^{\frac{1}{2}(\mu k + \nu l)} h_{k,l}$ in (6.1) yields

$$\frac{\partial^2 h_{k,l}}{\partial k^2} + \frac{\partial^2 h_{k,l}}{\partial l^2} - \frac{\mu^2 + \nu^2}{4} h_{k,l} = 0.$$

Changing to polar coordinates and setting $h(r, \theta) = u(r)v(\theta)$, we obtain, after rescaling r by $\sqrt{\mu^2 + \nu^2}/2$,

$$r^2 u''(r) + r u'(r) - (r^2 + n^2) u(r) = 0, \tag{6.2}$$

where n is to be determined, and

$$v''(\theta) + n^2 v(\theta) = 0.$$

Imposing $v(\theta) = 0$ for $\theta = 0$ and $\pi/2$ leads to $v(\theta) = \sin 2\theta$, hence $n = 2$. The solution of the differential equation for $u(r)$ is the Bessel function

$$u(r) = K_2\left(\sqrt{\mu^2 + \nu^2}\frac{r}{2}\right).$$

Finally, the solution, when $b \to 0$, reads, up to a normalizing constant,

$$f(r, \theta) = K_2\left(\sqrt{\mu^2 + \nu^2}\frac{r}{2}\right) \exp\left(\frac{r}{2}(\mu \cos\theta + \nu \sin\theta)\right) \sin 2\theta. \tag{6.3}$$

This solution encompasses all three regimes where $\mu r \sim 1$, $\mu r \ll 1$, or $\mu r \gg 1$. Simplified expressions are obtained in the two latter cases:

- For small values of the argument, we have $K_2(x) \sim 1/x^2$. We thus find
$$f(r, \theta) \approx \text{const}\, r^{-2} \sin 2\theta, \qquad (\mu r \ll 1),$$
which matches consistently with the critical solution (5.5) for $b \to 0$.
- For large values of the argument, we have $K_2(x) \approx \sqrt{\pi/2x}\, \mathrm{e}^{-x}$; hence we obtain the asymptotic behaviour
$$f(r, \theta) \approx \text{const}\, r^{-1/2}\, \mathrm{e}^{-rP(\theta)} \sin 2\theta, \qquad (\mu r \gg 1), \tag{6.4}$$
where
$$P(\theta) = \tfrac{1}{2}\left(\sqrt{\mu^2 + \nu^2} - \mu \cos\theta - \nu \sin\theta\right). \tag{6.5}$$

For any values of μ and ν non-simultaneously positive, $P(\theta)$ is positive, f is exponentially decaying, corresponding to a fluid phase. When μ and ν are simultaneously positive, $P(\theta)$ vanishes at an angle θ satisfying $\tan\theta = \nu/\mu$. For such a value of θ, the function $f(r, \theta) \sim r^{-1/2}$ is not normalizable. The whole region $\mu > 0$ and $\nu > 0$ is therefore non-physical.

6.2. Stationary solutions at exponential order: discrete equation

In order to investigate exponentially decaying solutions beyond the continuum limit, we consider the discrete equation (4.2) at stationarity. As above, for k and l large, we can neglect terms containing b, thus obtaining

$$f_{k+1,l} + f_{k,l+1} + \bar{u} f_{k-1,l} + \bar{v} f_{k,l-1} - (2 + \bar{u} + \bar{v}) f_{k,l} = 0. \tag{6.6}$$

Introducing the generating function $\hat{f}(x, y) = \sum f_{k,l} x^k y^l$, we get from (6.6)

$$D(x, y)\hat{f}(x, y) = A(x, y), \tag{6.7}$$

where

$$D(x, y) = x^{-1} + y^{-1} - 2 + \bar{u}(x - 1) + \bar{v}(y - 1). \tag{6.8}$$

The locus of singularities of $\hat{f}$ is thus given by $D(x, y) = 0$. The right-hand side, $A(x, y)$, comes from the contribution of the boundary terms $\hat{f}(0, y)$ and $\hat{f}(x, 0)$,[3]

$$A(x, y) = \hat{f}(0, y)\left(\frac{1}{x} - 1\right) + \hat{f}(x, 0)\left(\frac{1}{y} - 1\right).$$

By inversion we have

$$f_{k,l} = \oint \frac{\mathrm{d}x}{2\mathrm{i}\pi x} \frac{\mathrm{d}y}{2\mathrm{i}\pi y} \hat{f}(x, y) x^{-k} y^{-l}.$$

At large k and l, $f_{k,l}$ can be estimated by taking the saddle point of this expression, yielding

$$f_{k,l} \sim x^{-k} y^{-l} \equiv \mathrm{e}^{-r P(\theta)},$$

where x, y is a point on the curve $D(x, y) = 0$, and $P(\theta) = \cos\theta \ln x + \sin\theta \ln y$. Extremizing $P(\theta)$ on this curve with respect to the variables x and y, i.e. the expression $P(\theta) - \lambda D(x, y)$, where λ is a Lagrange multiplier, leads, together with $D(x, y) = 0$, to three equations, which determine λ, x and y, hence $P(\theta)$.

Let us first check that this method leads to the expected result (6.5) in the particular case of the continuum limit. Set $x = \mathrm{e}^s$, $y = \mathrm{e}^t$, $\bar{u} = \mathrm{e}^\mu$, $\bar{v} = \mathrm{e}^\nu$, with μ and ν being small. The equation for $D(x, y)$ reads

$$s^2 + t^2 + \mu s + \nu t = 0.$$

Extremizing $P(\theta) - \lambda D(x, y)$ with respect to s and t yields

$$\lambda \cos\theta - 2s + \mu = 0, \qquad \lambda \sin\theta - 2t + \nu = 0.$$

The three former equations lead, after some algebra, to equation (6.5).

The general case leads to lengthy expressions for $P(\theta)$. We give the results of this method for a particular example. We choose $\bar{u} = 1.89$, $\bar{v} = 0.66$ in the stationary equations, which we integrate by solving the linear system, as explained in section 5.2, for increasing values of the cut-off $m_\star$. The resulting values of the densities ρ_1 and ρ_2 are plotted in figure 3. Clearly

[3] For the generic case $b > 0$, $A(x, y)$ is finite on $D(x, y)$, while if $b = 0$, the singularities of $A(x, y)$ cancels those of $D(x, y)$ in such a way that the resulting expression for $\hat{f}(x, y)$ has just a simple pole in both complex variables x and y:

$$\hat{f}(x, y) = \frac{(1 - \bar{u})(1 - \bar{v})}{(1 - \bar{u}x)(1 - \bar{v}y)}, \qquad (b = 0).$$

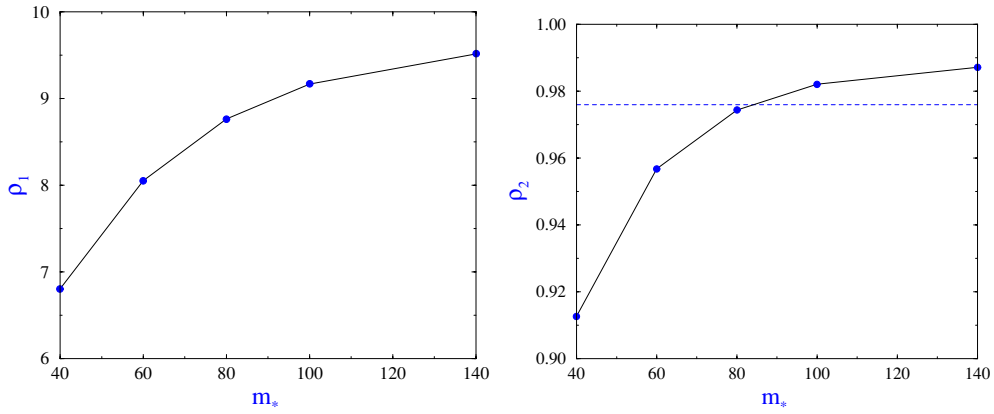

Figure 3. Densities as functions of $m_\star$ ($\bar{u} = 1.89, \bar{v} = 0.66, b = 3/2$). The dashed line corresponds to ρ_c.

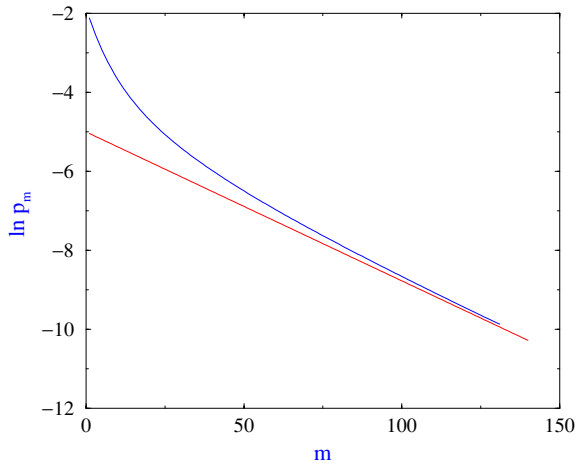

Figure 4. Distribution of the total single-site occupation p_m as a function of m ($m \leqslant m_\star = 140$). Line: theoretical prediction for the coefficient of the exponential decay. ($\bar{u} = 1.89, \bar{v} = 0.66$, $b = 3/2$.)

ρ_2 is larger than ρ_c.[4] Figure 4 depicts $\ln p_m$, as obtained by the same method, together with the theoretical prediction for the coefficient of the exponential decay:

$$p_m = \int r\,\mathrm{d}r\,\mathrm{d}\theta\,\mathrm{e}^{-rP(\theta)}\delta\left(r - \frac{m}{\cos\theta + \sin\theta}\right) \sim \exp\left(-m\frac{P(\theta_0)}{\cos\theta_0 + \sin\theta_0}\right),$$

where θ_0 denotes the value of the angle such that the argument of the exponential is minimum. In the present case, $\theta_0 = 0$, and $p_m \sim \mathrm{e}^{-0.0372m}$.

[4] The values of $\bar{u}$ and $\bar{v}$ were precisely chosen to serve this purpose. We first integrated the master equation (4.2) numerically for $b = 3/2$, corresponding to $\rho_c \approx 0.976$, and for values of the densities $\rho_1 = 10$ and $\rho_2 = 1$. The stationarity values $\bar{u} \approx 1.894$, $\bar{v} \approx 0.661$ were thus obtained.

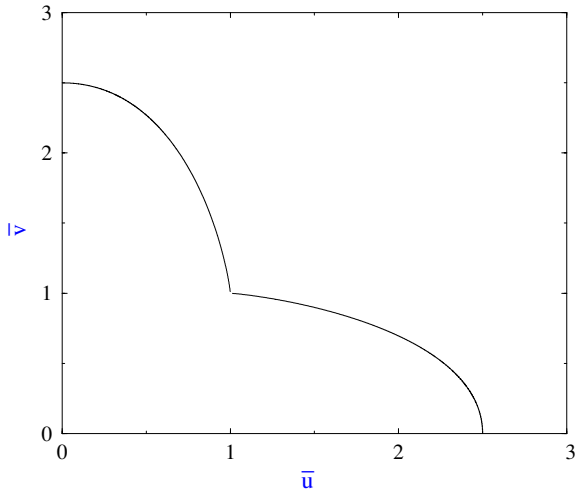

Figure 5. Domain of existence of the homogeneous fluid solution ($b = 3/2$). The lower right wing corresponds to $\rho_1 = \infty$, ρ_2 finite, and symmetrically for the left upper wing.

6.3. Domain of existence of the fluid phase in the $\bar{u} - \bar{v}$ plane

The domain of existence of the homogeneous fluid solution in the $\bar{u} - \bar{v}$ plane is shown in figure 5. It is the interior of the domain delimited by the two symmetric curves. These curves are obtained as follows. Consider the situation where one of the densities, ρ_1, say, is infinite. Then $v_{k,l}$ is to be taken equal to 1, and it is intuitively expected that the two species decouple. Hence $f_l = (1 - \bar{v})\bar{v}^l$. It follows that

$$\rho_2 = \frac{\bar{v}}{1 - \bar{v}},$$

and

$$\bar{u} = \sum_{l=0}^{\infty} f_l \left(1 + \frac{b}{l}\right) = 1 + b(1 - \bar{v})(1 - \ln(1 - \bar{v})). \tag{6.9}$$

The two former equations give the equation of the boundary of the domain of existence of fluid solutions, for ρ_2 varying. The second part of the curve is obtained symmetrically by doing the same analysis with ρ_2 infinite. We note that the tangents to the two curves at the symmetric point $\bar{u} = \bar{v} = 1$ are parallel to the axes.

6.4. Limits of stability of the fluid phase

Finally the question is how the domain of existence of the fluid region defined above is mapped onto the density plane. As we now show, this domain maps onto a region of the density plane complementary to a wedge with tip located at the critical point $\rho_1 = \rho_2 = \rho_c$, as depicted in figure 6. All the analysis relies on how the neighbourhood of the point $\bar{u} = \bar{v} = 1$ is mapped onto the density plane.

We begin by a linear analysis of the mapping between the critical points ($\bar{u} = \bar{v} = 1$) and ($\rho_1 = \rho_2 = \rho_c$). Consider a small segment, with one of the two ends located at $\bar{u} = \bar{v} = 1$, and with the other one at a given angle with the $\bar{u}$ axis. Let t be the tangent of this angle. Because of the symmetry between the two species, and since the transformation of the local derivatives

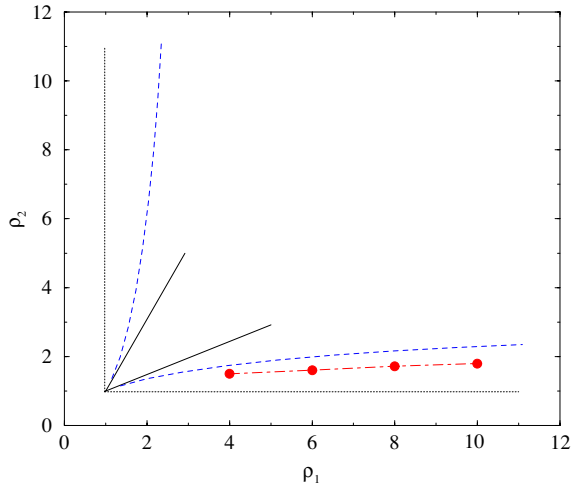

Figure 6. Phase diagram in the density plane. Dot-dashed line with circles: line of transition points (the symmetric line is not figured). Dashed lines: limits of stability of the fluid phase. Dotted lines: limits of stability of the condensed phase. Straight lines at the tip (critical point) are the local tangents, computed as explained in the text. ($b = 3/2$, $\rho_c \approx 0.976$.)

around the critical point is linear, the slope of the transformed segment in the density plane is given by

$$T = \frac{1 + ct}{c + t}. \tag{6.10}$$

Thus, if $t = \pm 1$, then $T = \pm 1$. The constant c is determined numerically by taking $t = \infty$ (segment parallel to the $\bar{v}$ axis). The limiting slopes of the tangents to the wedge at the tip follow from (6.10). For the lower edge it is given by $T(t = 0)$, i.e., $1/c$. For $b = 3/2$, we find $T(t = 0) \approx 0.48$, with $m_\star = 80$.

We then investigate how points located on the boundary curve (6.9), at increasing distances of the critical point, $\bar{u} = \bar{v} = 1$, are mapped onto the density plane. For successive values of the cut-off $m_\star$ the images of these points are expected to converge to a single curve. The lower edge of the wedge depicted in figure 6 is the curve with $m_\star = 160$. The other edge is obtained by symmetry. These edges represent the limits of stability of the fluid phase.

7. Condensation and phase diagram

As shown in the previous section, fluid solutions of (4.2) and (5.1) exist in the region of the density plane complementary to a wedge delimited by the limits of stability of the fluid phase. On the other hand, one expects *a priori* a condensate to exist whenever both of the densities are larger than the common critical density ρ_c. Anticipating on what follows, we name the line $\rho_2 = \rho_c$, $\rho_1 > \rho_c$, and the symmetric line with respect to the bisectrix, the limits of stability of the condensed phase. The question is now to determine whether those solutions (both fluid and corresponding to a condensate) are physical, i.e., that they have a finite basin of attraction. This question can only be approached in the present context by Monte Carlo simulations.

7.1. Equal densities

The case of equal densities, $\rho_1 = \rho_2$, is similar to the situation encountered for a single-species ZRP [3, 4]. From the analysis of the previous sections, as well as from numerical integrations of the temporal equations (4.2), or of their stationary form, and of Monte Carlo simulations, the following picture is obtained.

The region $\bar{u} = \bar{v} < 1$ maps onto the fluid phase $\rho_1 = \rho_2 < \rho_c$, corresponding to exponential solutions of equation (5.1). The critical point corresponds to $\bar{u} = \bar{v} = 1$, i.e., $\rho_1 = \rho_2 = \rho_c$. Condensation occurs for $a > 3$,[5] i.e. $b > 2/3$ (see equation (5.6)), and $\rho_1 = \rho_2 > \rho_c$. A condensate appears sustaining the excess density with respect to the critical fluid. The region $\bar{u} = \bar{v} > 1$ is unphysical.

7.2. Nonequal densities: existence of a line of transition

The aim of this section is to give an account of the numerical evidence for the existence of a transition line between the fluid phase and the condensed phase, lying in between the two corresponding stability lines of these phases. The transition is discontinuous on the transition line. There is no coexisting solutions accessible dynamically on both sides of the line.

The transition between the fluid and condensed phases is obtained by Monte Carlo simulations of the model, using the following procedure. The density ρ_1 is fixed to a given value greater than ρ_c, and ρ_2 increases from a value less than ρ_c. Crossing the stability line of the condensed phase, i.e. for $\rho_2 > \rho_c$, one might expect condensation to occur. Instead, the only accessible phase turns out to be the fluid one (see an example of fluid solution in section 6.2). Then, increasing the density ρ_2, and crossing the transition line, there is a sudden phase transition from an imbalanced fluid where the two species have different densities, both larger than the critical density, to a neutral critical fluid and an imbalanced condensate, i.e. with different number of particles for the two species. Beyond this line, the only accessible solutions are condensed, with $\bar{u} = \bar{v} = 1$, while fluid solutions to equation (4.2) do exist[6], as long as ρ_2 has not reached the edge of the wedge. A surprising consequence of this phase diagram is the occurrence of a re-entrance phenomenon: increasing ρ_2 beyond the symmetric transition line (with respect to the bisectrix) the system becomes fluid again.

We now describe more precisely the method for the determination of the location of the transition line. We fix the value of ρ_1, for example $\rho_1 = 10$, and let ρ_2 increase from a value less than ρ_c. Then $\bar{u}$ and $\bar{v}$ are measured. Focussing on $\bar{u}$, we observe that, when ρ_2 crosses some value, $\rho_2 \approx 1.8$; there is a sudden discontinuity in $\bar{u}$, dropping from $\bar{u} \approx 1.4$ down to $\bar{u} \approx 1$. More precisely, for a system of given size, say $M = 40, 60, \ldots$, the system is first run to stationarity. Then n successive runs of duration Δt less than the flipping time τ between the fluid and the condensed phases, and such that $n\Delta t \gg \tau$ are performed. This flipping time is measured to be exponentially increasing with the system size (it is approximately doubled when M is incremented by 20). The histogram of the values of $\bar{u}$ is a bimodal distribution. The criterion for the location of the transition point (ρ_1^*, ρ_2^*), when ρ_2 varies, consists in choosing the value of ρ_2 such that the two weights of the two maxima are equal. Thus for $M = 40, 60, 80$, we have $\rho_2^* \approx 1.86, 1.82, 1.8$, respectively.

We proceed in the same fashion to obtain the transition points visible in figure 6, for $\rho_1 = 4, 6, 8$. As ρ_1 decreases down to ρ_c, the discontinuity in $\bar{u}$ is smaller and the determination of the transition point is harder since it involves larger system sizes.

[5] The condition for condensation is that the decay exponent of $f_k \sim k^{a-1}$ be larger than 2 (see, e.g. [3, 4]).

[6] These solutions are difficult to obtain practically. This is so because the method employed above (for the case $\bar{u} = 1.89$, $\bar{v} = 0.66$) is not adequate here. The temporal master equation is in a regime of slow coarsening and hence the convergence of $\bar{u}$ and $\bar{v}$ to their stationary values is very slow.

Let us finally come back on the definition given at the beginning of this section for the limits of stability of the condensed phase. They were introduced in the present situation by analogy with the case of static first order phase transitions, where the transition takes place between two spinodals. In practice, it is likely that a condensate outside the condensed phase region will be unstable for any finite system.

8. Final remarks

Let us first summarize the main outcomes of the present work. For the process considered, a non-integrable two-species ZRP, we are able to obtain a number of analytical results from the study of the model on the complete graph. In particular the critical phase is well understood. The coefficient of the exponential decay of the fluid solutions is analytically predicted. Finally we can predict the phase diagram of the system by a joint analytical and numerical investigation. A salient feature of the phase diagram is the presence of a single critical point. A more thorough analysis of the first-order phase transition taking place between the fluid phase and the condensed phase would be interesting, though probably hard to achieve. The existence of such a transition is not expected in integrable two species ZRP [9, 10, 13, 14]. In the latter case, it is known that the domain of existence of the homogeneous fluid solution is convex in the fugacity plane [14]. In the present case, this domain is not convex in the $\bar{u} - \bar{v}$ plane (cf figure 5).

Beyond the present work, a natural question to ask is whether the phenomena observed for the fully connected geometry survive in the one-dimensional geometry. Preliminary investigations using the analysis performed on the complete graph as a template indicate similar behaviour.

Acknowledgments

It is a pleasure to thank J-M Luck for invaluable discussions. Thanks are also due to E G D Cohen, M Evans, S Grosskinsky, T Hanney, E Levine and D Mukamel for helpful discussions. This work was partially carried out while CG was a Meyerhoff Visiting Professor at the Weizmann Institute. Support of the Albert Einstein Minerva Center for Theoretical Physics and the Israel Science Foundation (ISF) is gratefully acknowledged.

References

[1] Spitzer F 1970 *Adv. Math.* **5** 246
[2] Kipnis C and Landim C 1999 *Scaling Limits of Interacting Particle Systems* (Berlin: Springer)
[3] Evans M R and Hanney T 2005 *J. Phys. A: Math. Gen.* **38** R195
[4] Godrèche C 2006 *Aging and the Glass Transition* ed M Henkel, M Pleimling and R Sanctuary (*Springer Lecture Notes in Physics* to be published) *Preprint* cond-mat/0604276
[5] Kafri Y, Levine E, Mukamel D, Schütz G M and Török J 2002 *Phys. Rev. Lett.* **89** 035702
[6] Godrèche C, Levine E and Mukamel D 2005 *J. Phys. A: Math. Gen.* **38** L523
[7] Andjel E D 1982 *Ann. Probab.* **10** 525
[8] For a short review, see Godrèche C and Luck J-M 2002 *J. Phys. Condens. Matter* **14** 1601
[9] Grosskinsky S and Spohn H 2003 *Bull. Braz. Math. Soc.* **34** 489
[10] Evans M R and Hanney T 2003 *J. Phys. A: Math. Gen.* **36** L44
[11] Kolmogorov A N 1936 *Math. Ann.* **112** 115
[12] Kelly F 1979 *Reversibility and Stochastic Networks* (New York: Wiley)
[13] Hanney T and Evans M R 2004 *Phys. Rev.* E **69** 016107
[14] Grosskinsky S in preparation